Sensors and Actuators B 251 (2017) 49–56

Contents lists available at ScienceDirect

Sensors and Actuators B: Chemical

journal homepage: www.elsevier.com/locate/snb

Diketopyrrolopyrrole copolymers based chemical sensors for the detection and discrimination of volatile organic compounds

Bin Wang[a], Prashant Sonar[b,c,*], Sergei Manzhos[d], Hossam Haick[a,**]

[a] Department of Chemical Engineering and Russell Berrie Nanotechnology Institute, Technion-Israel Institute of Technology, Haifa 3200003, Israel
[b] School of Chemistry, Physics and Mechanical Engineering, Queensland University of Technology, GPO Box 2434, Brisbane, QLD 4001, Australia
[c] Institute of Materials Research and Engineering (IMRE), Agency for Science, Technology and Research (A*STAR), 3 Research Link, Singapore 117602, Singapore
[d] Department of Mechanical Engineering, National University of Singapore, Block EA #07-08, 9 Engineering Drive 1, Singapore 117576, Singapore

ARTICLE INFO

Article history:
Received 14 December 2016
Received in revised form 20 March 2017
Accepted 26 April 2017
Available online 29 April 2017

Keywords:
Semiconducting polymer
Diketopyrrolopyrrole
Organic field effect transistor
Sensor
Volatile organic compound

ABSTRACT

With their high charge carrier mobility and easy solution processability, diketopyrrolopyrrole (DPP) copolymers are considered as very promising active organic semiconducting materials for a wide range of organic electronic devices. This class of materials has already successfully demonstrated a very high mobility in organic thin film transistors (OFETs) and impressive performance in organic photovoltaic (OPV) devices. Apart from OFET and OPV, there are very few reports about these materials for other organic electronic devices such as chemical sensors. In the present work, we have used these high mobility DPP copolymers as active semiconductors in OFET device based chemical sensors for sensing of volatile organic compounds (VOCs) in air. Combined with a pattern recognition algorithm and sensor data obtained from an array of DPP copolymer OFETs, VOCs with similar structure can be discriminated from each other. This opens up a novel opportunity to use promising DPP based polymers as active semiconductors for chemical sensors.

1. Introduction

Aliphatic and aromatic volatile organic compounds (VOCs) such as volatile alkanes and benzene derivatives are widely used in fuels and solvents. However, their vapors are harmful to human health and cause various diseases [1]. In addition to their adverse effect on human health, these VOCs can react easily in atmosphere with nitrogen oxides (NO_x) and carbon monoxide (CO) in presence of sunlight and can form hazardous ground level ozone in the environment [2]. Therefore, detection of VOCs in the atmosphere is extremely important from the perspectives of environmental monitoring and public health.

Recently, conjugated organic semiconducting polymers have been considered as promising sensing materials because they: (i) can be processed into flexible low cost and large area devices using solution based fabrication technology; (ii) can self-assemble into nano- or micro-structures with various morphological features; and (iii) can serve as both the framework and the sensing antenna of sensors [3–5]. Organic semiconducting polymers based chemiresistors and organic field effect transistors (OFETs) have been successfully applied in the sensing of VOCs [6–12], ammonia [13–16], vapors of explosives [17,18], and nerve agents [19,20]. However, developing organic semiconducting polymers based sensors with high sensitivity and selectivity to meet the practical application is still a challenge.

Due to their merits of high charge carrier mobilities, ease of synthesis, tailor-made optoelectronic property control and solution processibility, semiconducting copolymers incorporating diketopyrrolopyrrole (DPP) units are promising materials in the application of unipolar/ambipolar OFETs and solar cells [21–31]. There are several reports on DPP based polymers for OFET and OPV devices but so far, there are very few reports about using DPP copolymers for sensing applications [32–34]. Additionally, most of reported sensing results are measured in inert nitrogen (N_2) atmosphere, whereas in this work, we have studied sensing performance of DPP copolymer sensors in the atmosphere of air. Such sensors are closer to the practical application and are rarely reported. In the present work, we report the sensing of VOCs, including aliphatic alkanes and aromatic benzene derivatives, in air, using DPP copoly-

* Corresponding author at: School of Chemistry, Physics and Mechanical Engineering, Queensland University of Technology, GPO Box 2434, Brisbane, QLD 4001, Australia.
** Corresponding author.
E-mail addresses: snoar.prashant@qut.edu.au (P. Sonar), hhossam@tx.technion.ac.il (H. Haick).

http://dx.doi.org/10.1016/j.snb.2017.04.167
0925-4005/

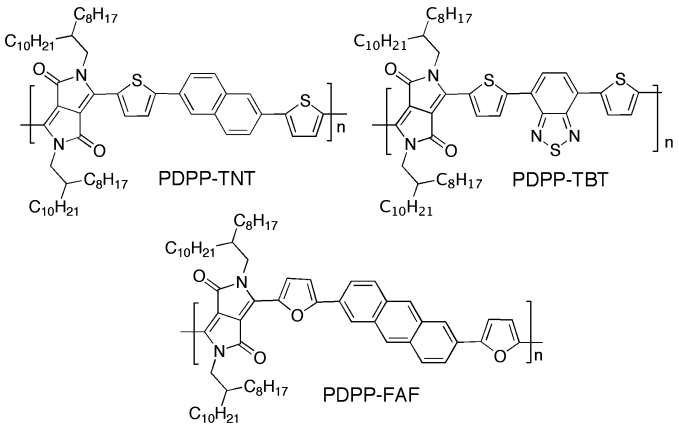

Scheme 1. Structure of DPP copolymers used in this study: PDPP-TNT, PDPP-FAF and PDPP-TBT.

mers based OFET, as well as quartz crystal microbalance sensing platform. Combined with a pattern recognition algorithm and sensor data obtained from an array of DPP copolymer based OFETs, VOCs with similar chemical structures can be distinguished. The polymers selected for OFET chemical sensor applications are PDPP-TNT, PDPP-FAF and PDPP-TBT. Their chemical structures are given below (Scheme 1).

2. Experimental

2.1. Fabrication of DPP polymer based OFET

We have chosen two p-type copolymers, namely, PDPP-TNT and PDPP-FAF comprised of electron accepting DPP with electron donating naphthalene and anthracene in the backbone, whereas the third polymer is an ambipolar copolymer PDPP-TBT constituted using DPP and benzothidiazole acceptor in the main chain. The idea behind using both p-type and ambipolar copolymers for OFET sensors is to demonstrate the versatility of these classes of donor-acceptor polymers for chemical sensor devices. All three copolymers were synthesized via Suzuki-coupling polymerization and reported previously [23,26,35]. The OFETs were prepared on a silicon (100) wafer capped with 300 nm SiO_2. The Ti/Au (10/200 nm) bottom gate electrode was deposited by electron beam evaporation. 49 pairs of interdigitated concentric ring source and drain Ti/Au (30/200 nm) electrodes with a 25 μm gap between two adjacent electrodes were prepared using photolithography and electron beam evaporation, respectively (Fig. 1a). The silicon wafers were treated in an oxygen plasma for 5 min followed by immersing in octyltrichlorosilane (OTS) in toluene (40 mM, 20 mL) for 10 h in a N_2 glove-box for self-assembled monolayer (SAM) treatment. The thin films of PDPP-FAF, PDPP-TNT, and PDPP-TBT polymers were deposited on the OTS treated Si/SiO_2 substrates by spin coating using a polymer solution in chloroform (8 mg/mL). Finally, polymer OFETs were annealed at 135 °C for 30 min in N_2 glove-box. A scanning electron microscopy (Zeiss Ultra-Plus FEG-SEM) was applied to measure the morphology of DPP copolymer films on OFETs.

2.2. OFET sensor characterization

Two groups of VOCs: aliphatic alkanes (hexane, octane, and decane) and aromatic benzene derivatives (benzene, toluene, and p-xylene) were used as analytes in this study. These chemicals are widely used in fuels and solvents. However, their vapors are harmful to human health and are considered as major source of urban air pollution. The vapors of VOCs were generated by a computer-controlled bubbler system. Oil-free purified dry air was used as the carrier gas for the analytes as well as the reference gas. In this study, three concentrations of vapor in air, $P_a/P_o = 0.05$, 0.1, and 0.2 were used, where P_a stands for the partial pressure of the analytes and P_o is the saturated vapor pressure. OFET sensors were loaded into a stainless steel chamber with a ~170 cm^3 volume and measured with a Keithley 2636A system SourceMater and a Keithley 3706 system Switch/Multimeter under a 5 L/min constant flow. All OFET devices were measured under the hole accumulation mode. During the OFET measurement, the source-drain voltage (V_{ds}) was kept at 20 V, and the gate voltage (V_g) was swept between 0 and −70 V with 200 mV steps.

2.3. Data analysis

Relative changes of the source-drain current (I_{ds}) at $V_g = -70$ V and relative changes in hole mobility were used as sensing signals of DPP copolymer based OFET sensors. Principle component analysis (PCA) was performed using the JMP 10 software.

2.4. Quartz crystal microbalance (QCM) – polymer hybrid sensor

In addition to the OFET devices, we also fabricated quartz crystal microbalance devices using PDPP-FAF, PDPP-TBT, and PDPP-TNT polymers. The polymer solutions of all three copolymers in chloroform (8 g/mL) were spin coated on the gold plated QCM resonators and then annealed in a N_2 glove-box at 135 °C for 30 min using identical annealing conditions to those used for OFET devices to compare the chemical sensor response and performance. QCM sensors were tested by a LibraNose system (Technobiochip, Italy) under a 0.4 L/min constant flow. Sensing signals of QCM sensors were collected for 15 min under dry air flow, followed by 15 min under VOC vapor flow. Changes of mass upon exposure to VOCs were calculated by the shift of sensor resonant frequency.

2.5. Ab initio calculations

Calculations were performed using the Density Functional Theory (DFT) method [36,37] and Gaussian 09 software [38]. The range-separated and dispersion-corrected functional ωB97XD was used [39,40]. The basis set was 6-31g(d,p). In view of the weak interactions considered here, we also tested 6-31g+(d,p) with diffuse functions. Although the addition of the diffuse basis functions lowered total energies and the energies of frontier orbitals by tenths of an eV, the interaction energies are within 0.1 eV from those with 6-31g(d,p) while the convergence could not be achieved for some systems with 6-31g+(d,p). We therefore report data obtained with 6-31g(d,p). Calculations were performed in vacuum which was appropriate for the purpose of confirming the mechanism of intermolecular interactions.

3. Results and discussions

3.1. Characterization of DPP copolymers based OFET sensors

In this study, three polymers, PDPP-TNT, PDPP-FAF, and PDPP-TBT, which have the thiophene and furan flanked DPP segment with naphthalene, anthracene and benzothiadiazole comonomer units were selected as the active sensing materials for the detection and classification of aliphatic and aromatic VOCs (Scheme 1). These polymers are easily solution processable and can be dissolved in common organic solvents due to the long branched alkyl chain substituted on the lactam nitrogen atom of the DPP unit. It was also anticipated that the branched alkyl side chains have a high affinity toward the alkane analytes whereas the main chain conjugated backbone is favorable for the adsorption of aromatic analytes.

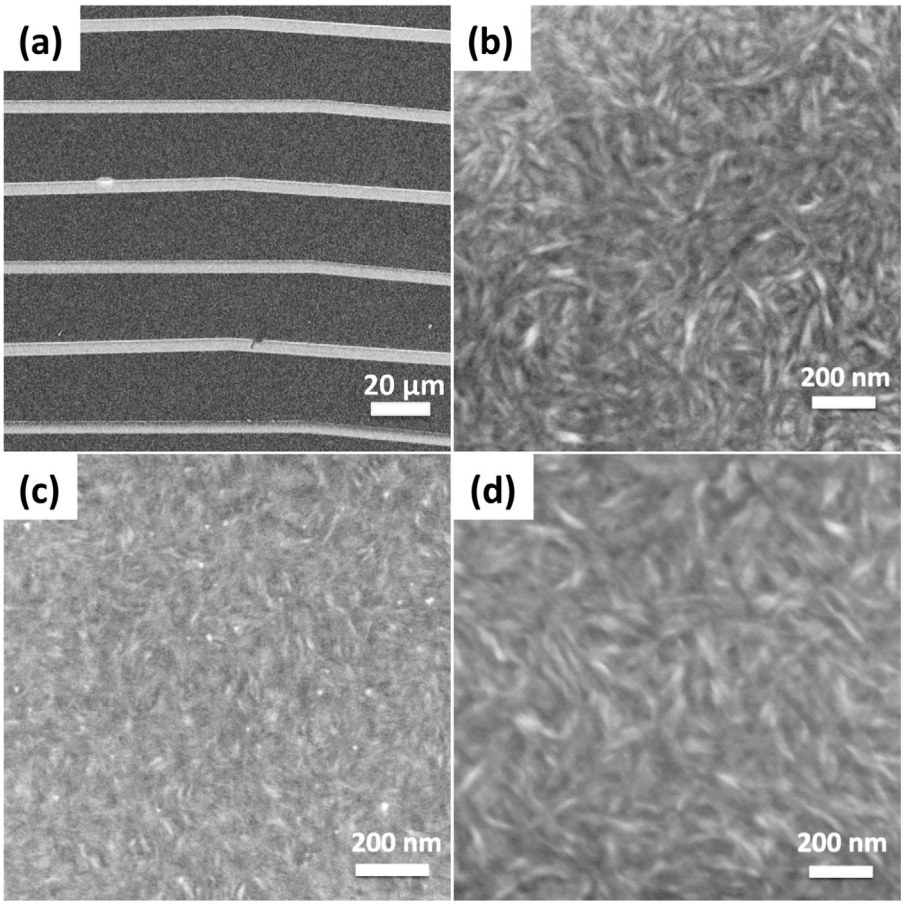

Fig. 1. (a) Scanning electron microscopy (SEM) image of a typical OFET surface (white lines are segments of the interdigitated concentric ring electrodes). SEM images of (b) PDPP-TNT, (c) PDPP-FAF, and (d) PDPP-TBT thin films after annealing at 135 °C on Si wafer surface.

These DPP copolymers involve fused aromatic rings with extended donor and acceptor comonomers such as naphthalene, anthracene or benzothiadiazole in the backbone. Such donor-acceptor copolymers with a large overlapping area have a strong tendency to form π–π stacks and assemble to interconnected network of nanofibers in the solid phase. We have analyzed these copolymers by Scanning Electron Microscopy (SEM) and as per shown SEM images (Fig. 1b and d), each fiber is about 10–30 nm in width. The nanofiber networks of these polymer films not only form highly efficient charge transport conducting pathways for charge-carrier mobility enhancement, but also provide a larger surface area like any other nanomaterials, which facilitates the adsorption of VOCs on polymer film surface.

Further, we integrated these semiconducting polymers into OFET devices and studied changes in their electrical properties upon exposure of various vapors of alkanes and aromatic compounds. During the OFET sensing measurements, a series of I_{ds} vs V_g electrical characteristics were collected. Fig. 2a shows a group of I_{ds} vs V_g curves of PDPP-TNT OFET sensors upon exposure to different concentrations of benzene. For V_g values between about −55 and −70 V, the I_{ds} gradually decreased as the benzene concentration increases from $P_a/P_o = 0$ (absence of benzene) to 0.2. Two sensing parameters were extracted: (i) the change in I_{ds} current at $V_g = -70$ V; and (ii) hole mobility (μ), which is extracted from the linear part of I_{ds} vs V_g curve. Note that more sensing parameters, such as I_{ds} at different V_g, can be extracted from I_{ds} vs V_g curves. Here we only consider two parameters most closely relevant to the typical sensing response of polymer OFET sensors.

3.2. Sensing responses of DPP copolymer based OFET sensors toward analytes

Fig. 2b and c represents the normalized response, $\Delta\mu/\mu_0$ and $\Delta I/I_0$ of DPP copolymer OFETs to the successive concentrations of benzene. μ_0 and I_0 are the baseline mobility and current of sensor in dry air; $\Delta\mu$ and ΔI are the mobility and current change upon analyte exposure. Upon expose to benzene, $\Delta\mu/\mu_0$ and $\Delta I/I_0$ decreased and their amplitudes were dependent on the benzene concentration. When the flow changed to dry air, $\Delta\mu/\mu_0$ can nearly revert to the original value. However, the $\Delta I/I_0$ has a small drift after the benzene exposure. This suggests that the two sensing parameters are independent on each other.

The sensing responses of DPP copolymer OFET sensors toward different concentrations of VOCs are summarized in Fig. 3. All the sensors show negative response in $\Delta\mu/\mu_0$ and $\Delta I/I_0$ upon exposure to VOCs. Sensing responses in mobility and current are increased with VOC concentration for all the test sensors. Upon exposure to alkanes, the PDPP-TNT OFET shows the largest response in mobility and current in most cases, followed by the PDPP-TBT OFET. The PDPP-FAF OFET shows the weakest response to alkane VOCs. The exceptional case is the sensing response in current toward hexane, where the PDPP-TBT OFET shows the largest sensing response. Upon exposure to aromatic VOCs, the PDPP-TNT OFET shows the largest response in mobility and current, followed by the PDPP-FAF OFET, then the PDPP-TBT OFET. Interestingly, the sensing responses in current of all the test sensors toward aromatic VOCs are increased with VOC molecular weight at higher VOC concentrations ($P_a/P_o = 0.1$ and 0.2, Fig. 3a). However, there is no clear

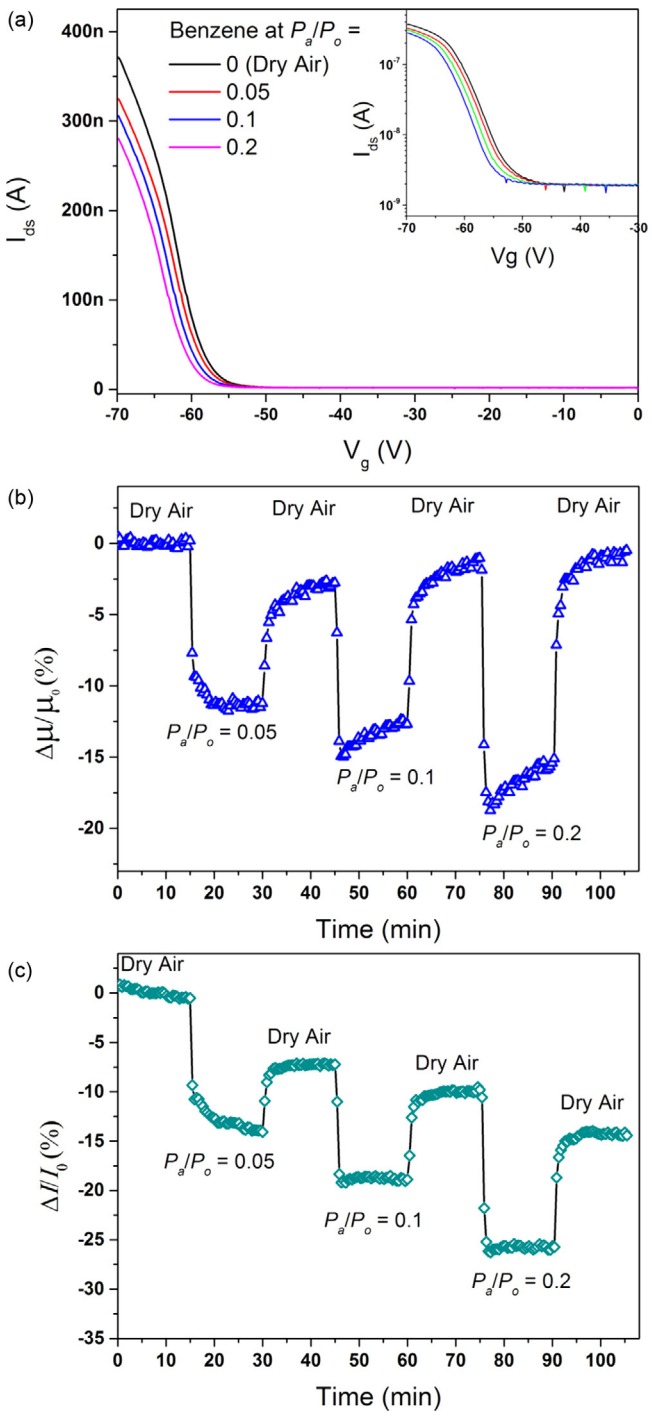

Fig. 2. (a) Linear and logarithmic scale (inset) I_{ds}–V_g curves of a PDPP-TNT OFET at different benzene concentrations. Time dependent response of a PDPP-TNT OFET upon expose to different concentrations of benzene as expressed by: (b) $\Delta\mu/\mu_0$ and (c) $\Delta I/I_0$.

VOC molecular weight dependent trend for the sensing responses of polymer OFET sensors toward alkanes. For all the polymer OFET sensors, the responses in $\Delta\mu/\mu_0$ and $\Delta I/I_0$ to aromatic compounds are always larger than that to alkanes with the same carbon number (for example, Hexane vs Benzene). Such a strong response to aromatic compounds is due to the aromatic conjugated backbone present in the polymer structure which may have high affinity toward aromatic analytes.

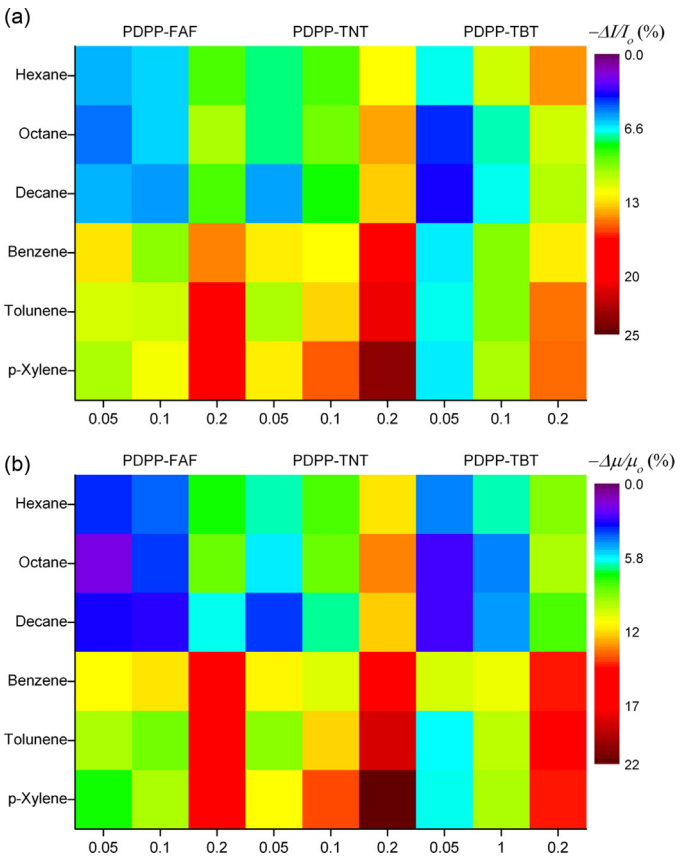

Fig. 3. Image plots of changes in (a) $\Delta\mu/\mu_0$ and (b) $\Delta I/I_0$ of three DPP copolymer OFET sensors upon exposure to various VOCs at different concentrations.

3.3. DPP copolymer OFETs for VOC discrimination

Selective detection of analytes with smaller chemical structure is highly demanded in many areas of sensor application. Generally, selectivity can be achieved by the so called “lock-and-key” approach, where a specific and strong interaction between the target analyte and the sensor surface, such as antibody–antigen combination, is required [41]. An alternative approach is using arrays of non-specific and cross-reactive sensors, followed by data processing of sensing signals using a pattern recognition algorithm to achieve selective sensing of target analytes [42]. This approach mimics the human olfaction system, therefore it is also called “electronic nose”. The electronic nose does not require specific interactions between the analyte and the sensor surface, therefore, it can simplify the sensor design.

We tested discriminative abilities of a DPP copolymer OFET array, by exposing three OFETs simultaneously to hexane, octane, decane, benzene, toluene, and p-xylene at a concentration of $P_a/P_o = 0.1$. For a given VOC, the three DPP copolymer OFET sensors generate six sensing features that form a fingerprint for identification of such VOC. Fig. 4a presents the principle component analysis (PCA) of the sensing response of the polymer OFET array upon analyte exposure. All tested VOCs produced distinctive signal response patterns by forming well-separated clusters in the principle component space. Furthermore, the results showed that the values of principal component 1 (PC1) for alkanes were all negative and PC1 values for aromatic compounds were all positive. In each group, individual analyte species were perfectly discriminated as well.

Increasing the number of sensors in a sensor array is believed to enhance the discrimination power for a set of analytes. However, it also increases the cost and complicates the sensor design [43,44]. To

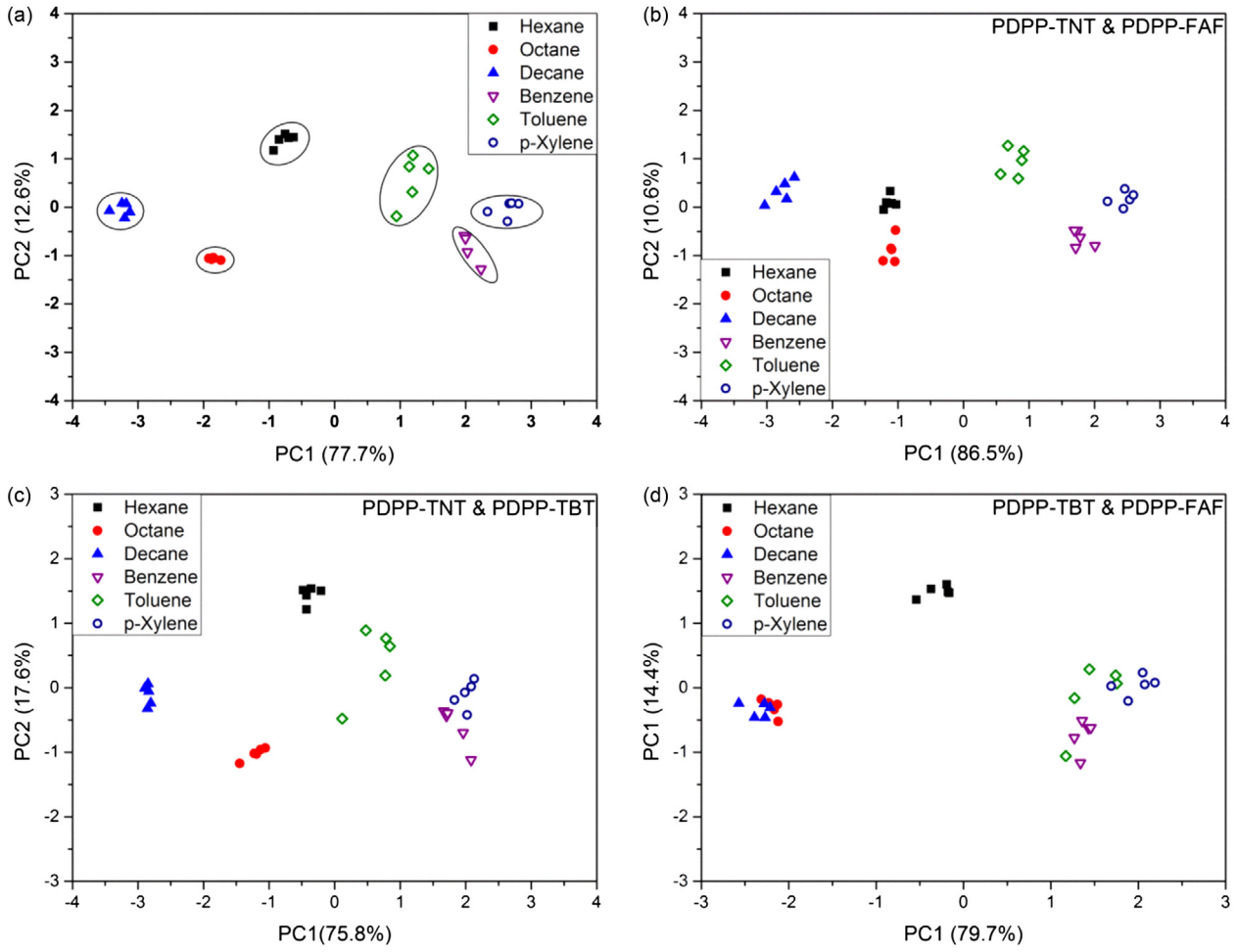

Fig. 4. Principle component score plot of an array of (a) 3 DPP copolymer OFETs and (b–d) 2 DPP copolymer OFETs upon exposure to VOCs (P_a/P_o = 0.1). Every data point corresponds to the group of sensing signals of selected sensors to a specific analyte.

minimize the sensor array and preserve the discrimination power, we applied the PCA analysis to an OFET sensor array that utilized two sensors. The results show that an array of only two DPP copolymer OFETs discriminates quite well between (i) the alkanes and aromatic compounds, (ii) between different alkanes, and even (iii) between different aromatic compounds (the case in PDPP-FAF and PDPP-TNT on the basis of their best performance), i.e. has a discriminating ability similar to that obtained with three sensors (Fig. 4b–d). The different combination of sensors has different discrimination power toward the tested VOCs. Specifically, the sensor array with PDPP-TNT and PDPP-FAF OFETs kept near the same power to discriminate all of the tested VOC spices. However, the sensor array with PDPP-TBT and PDPP-FAF can only discriminate between alkanes and aromatic compounds but failed to discriminate between VOC species. Thus, the data of sensor array discrimination power can be further used to screen high performance sensors and optimize sensor arrays to enhance the selectivity to target VOCs.

3.4. Sensing mechanism of DPP copolymer based OFET sensors

To study the interaction between VOCs and DPP copolymers, QCM sensors coated with polymer thin films were prepared. The mass change (Δm) of QCM sensor after VOC exposure is calculated by the Sauerbrey equation

$$\Delta m = -C_f A \Delta f \quad (1)$$

where C_f is the mass sensitivity (=1.104 ng cm^{-2} Hz^{-1}), A is the active area of the QCM resonator (=0.2 cm^2), and Δf is the change in frequency of quartz crystal resonator. As an example, Fig. 5a presents Δm (the mass change upon VOC exposure, where dry air exposure step is the baseline) of a bare QCM (without polymer coating) and polymer QCM hybrid sensors to successive concentrations of benzene. As shown in the figure, the bare QCM sensor produced a weak change in the Δm upon exposure to benzene, whereas DPP copolymer thin film deposited samples exhibit a dramatic enhancement in Δm value and the response in Δm increases as benzene concentration increases. The Δm returns back to near the baseline after a flow of air, which suggests that the tested VOCs are mainly physically adsorbed on the polymer film surface. The Δm responses of all QCM-polymer hybrid sensors to different concentrations of alkanes and aromatic compounds are summarized in Fig. 5b. The sensing responses are concentration dependent, namely, the absorbed VOC mass increased on the QCM-polymer hybrid sensors surface as the VOC concentration increased. For all the tested VOCs, the PDPP-FAF sensor has the largest response in mass change; while the PDPP-TNT sensor shows the weakest response. At the same concentration, the response to aromatic compounds is larger than that to alkanes.

The applied polymers have the same DPP unit with branched alkyl chain, but differ in their comonomer units. The difference in intermolecular interactions of different DPP copolymers induces different polymer molecule packing. Among the applied DPP copolymers, PDPP-FAF has the largest π–π stacking distance

Table 1
Physical properties of applied DPP copolymers [23,26,35].

Polymers	M_n (g mol^{-1})	Hole mobility (cm^2 V^{-1} s^{-1})	Interlayer d-spacing distance (Å)	π–π stacking distance (Å)
PDPP-TNT	63,750	0.65	20.05	3.82
PDPP-TBT	42,400	0.22	21.5	3.73
PDPP-FAF	20,584	0.07	19.7	4.41

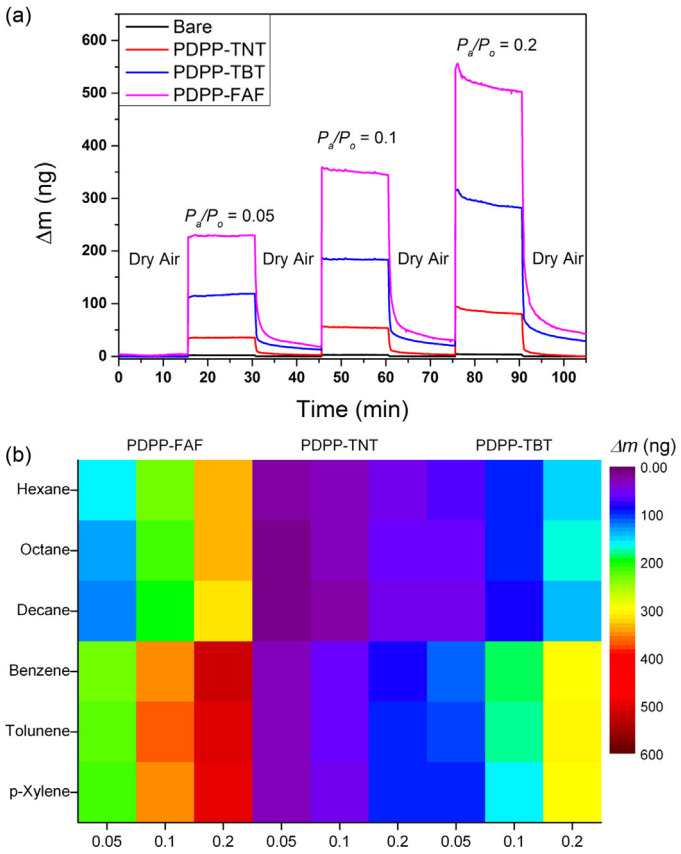

Fig. 5. (a) Changes in Δm of PDPP-TNT, PDPP-TBT, and PDPP-FAF/QCM hybrid sensors, as well as bare QCM sensor, upon exposure to different concentrations of benzene. (b) Changes in Δm of three DPP copolymer/QCM hybrid sensors upon exposure to various VOCs at different concentrations.

(4.41 Å, Table 1), indicting less packed polymer chains. The less packed polymer chains facilitate the diffusion and adsorption of VOCs in the free space inside the polymer nanofibers. In addition, PDPP-FAF forms nanofibers of smaller size, which offer a larger surface area for VOC adsorption (Fig. 1). Therefore, PDPP-FAF has the strongest VOC adsorption ability among the applied polymers, as revealed in the QCM experiment results (Fig. 5). Though the PDPP-FAF has the strongest adsorption ability toward VOCs, its OFET sensor shows the weakest response to the tested VOCs in most cases. It seems that the OFET sensor responses are more dependent on the hole mobility of the polymers (Table 1). PDPP-TNT has the largest hole mobility and its OFET sensor shows the strongest responses for most VOCs, while PDPP-FAF has the lowest hole mobility value and its OFETs shows the weakest responses for most VOCs. DPP copolymers have stronger affinity toward aromatic VOCs with pi-conjugation than aliphatic VOCs having non-conjugated nature because of the conjugated backbone of the DPP polymer chains. Therefore, DPP copolymers can adsorb larger amounts of aromatic VOCs than aliphatic VOCs, resulting in stronger sensing responses in change of mass and electric properties (Figs. 3 and 5b).

Table 2
Interaction energies (E_{int}) and frontier energy levels.

Molecule/complex	E_{int} (eV)	HOMO (eV)	LUMO (eV)
Benzene	n/a	−8.80	2.01
Hexane	n/a	−10.42	4.71
PDPP-TNT	n/a	−6.92	−0.84
Benzene on thiophene	0.28	−6.89	−0.83
Benzene on naphthalene	0.40	−6.89	−0.82
Benzene on DPP	0.52	−6.85	−0.78
Benzene on alkyl chain	0.34	−6.91	−0.83
Hexane on thiophene	0.34	−6.94	−0.85
Hexane on naphthalene	0.52	−6.92	−0.89
Hexane on DPP	0.67	−6.99	−0.93
Hexane on alkyl chain	0.40	−6.93	−0.86

After the VOC adsorption, DPP copolymer films will be swollen. The polymer film swelling will lead to a less tight contact between polymer nanofibers, resulting in an increase of contact resistance of the polymer film. In addition, the diffused VOCs inside the polymer nanofibers will also lead to a decrease in the order of polymer chain packing, resulting in a decrease in hole mobility. Therefore, hole mobility and current will decrease after VOC exposure, as was indeed seen in the polymer OFET exposure experiments (Fig. 2). Since the tested VOCs are nonpolar or weakly polar molecules, which have no strong charge transfer to DPP copolymers, the sensing responses are mainly from the swelling of the polymer films.

3.5. Molecular modeling

DFT simulations were used to further study the interactions between DPP copolymers and analytes. We chose one representative monomer, PDPP-TNT, and for analytes, one representative aromatic compound, benzene, and one representative alkane, hexane. Adsorption geometries and energies were computed by optimizing analyte-momoner complexes where initially the analytes were placed near the alkyl chains and near the aromatic moieties (naphthalene, thiophene as well as DPP). The resulting optimized configurations are shown in Fig. S1 and Fig. S2 (see Supporting Information), and the resulting adsorption energies are given in Table 2. Table 2 also lists highest occupied molecular orbital (HOMO) and lowest unoccupied molecular orbital (LUMO) energy levels of individual molecules as well as complexes. Mulliken charges on molecules were analyzed but did not show any intermolecular charge transfer.

The following conclusions can be drawn from Table 2. Firstly, all complexes represent physisorption. This is evidenced by a relatively weak magnitude of E_{int} (0.3–0.7 eV), the absence of charge donation between the interacting molecules, and the negligible perturbations to HOMO and LUMO levels in most cases. The only cases with any noticeable effect on the frontier orbitals is the adsorption of hexane on the DPP where both HOMO and LUMO are stabilized by about 0.08 eV and benzene over DPP where both HOMO and LUMO are destabilized by about 0.06 eV. Even in these cases there is no charge donation between the molecule and no effect on the nodal structures of HOMO and LUMO. They can therefore still be characterized as physisorption. The HOMO and LUMO isosurfaces are shown in Fig. 6 for pure PDPP-TNT and for the case of benzene adsorption on the naphthalene unit. They are visually

Table 3
Estimated limit of detection (LOD) of polymer OFET and QCM sensors, and health permissible exposure limit (PEL) to VOCs in ppm.

VOC	PEL	PDPP-FAF			PDPP-TNT			PDPP-TBT		
		LOD ($\Delta\mu/\mu_0$)	LOD ($\Delta I/I_0$)	LOD (Δm)	LOD ($\Delta\mu/\mu_0$)	LOD ($\Delta I/I_0$)	LOD (Δm)	LOD ($\Delta\mu/\mu_0$)	LOD ($\Delta I/I_0$)	LOD (Δm)
Hexane	500	10,251	10,077	**142**	3597	3011	**288**	3493	979	**179**
Ooctane	500	1628	**451**	**44**	**301**	**478**	**56**	**447**	**101**	**34**
Decane	500	**354**	**179**	**2**	**102**	**83**	**16**	**142**	**40**	**9**
Benzene	1	4992	2115	243	832	784	93	1108	470	56
Toluene	200	1245	905	**65**	361	201	**81**	481	**138**	**88**
p-Xylene	100	498	404	**39**	178	**62**	**39**	182	162	**47**

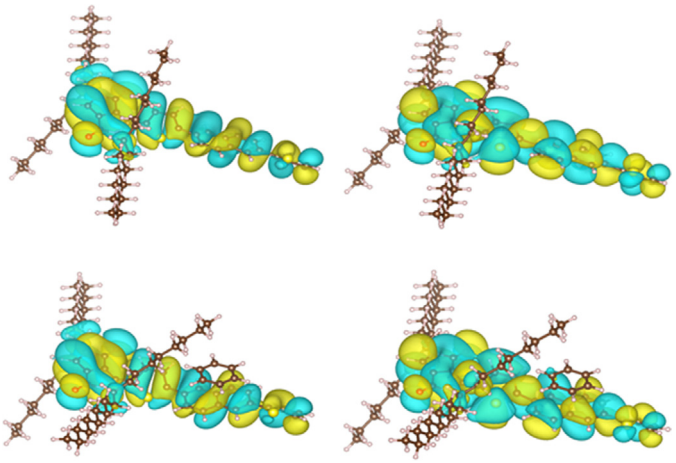

Fig. 6. The HOMO (left) and LUMO (right) isosurfaces for pure PDPP-TNT (top) and for the case of benzene adsorption on the naphthalene unit of PDPP-TNT (bottom).

similar for other cases and show negligible effect of the analyte on the shape of the frontier orbitals. Next, for both benzene and hexane, the adsorption is strongest on the DPP followed by on the fused ring, followed by the alkyl chain followed by thiophene. In the case of hexane coordinated to the DPP, the hexane is also interacting with the alkyl chain (Fig. 6) which must contribute substantially to its E_{int}. A similar situation is observed with benzene over the fused ring which also interacts with an alkyl chain of the monomer. These simulations therefore do not show the selectivity of aromatic moieties of the monomers to aromatic analytes and of alkyl chains for alkanes. This, however, could be due to the neglect by the model of crystal packing which can have a severe effect on interaction energies [45,46].

3.6. Limit of detection

LOD (limit of detection) for sensor is the lowest amount of quantity of analyte required to distinguish the difference between presence of analyte and absence of analyte (a blank value) within a given limit. LOD for the lower operating concentration of a sensor is generally accepted as the analyte concentration corresponding to a signal-to-noise (S/N) of three. In the practical application, sensors are required to be able to detect VOCs below the health permissible exposure limit (PEL). Therefore, a qualified sensor toward a VOC should have a LOD less than the PEL value. To evaluate their potential in practical application, LODs of OFET and QCM-polymer hybrid sensors toward VOCs were calculated and summarized in Table 3. The details of LOD calculation are described in Supporting Information. Additionally, US National Institute for Occupational Safety and Health (NIOSH) recommended PEL of VOCs are also listed in Table 3. The LOD value less than PEL have been marked bold. As shown in the table, the LODs of DPP polymer/QCM hybrid sensors are less than PEL for most VOCs, except benzene. However, for most VOCs, the estimated LOD of polymer OFETs are larger than PEL. For the same OFET device, LOD value estimated by $\Delta I/I_0$ is always less than that estimated by $\Delta\mu/\mu_0$, suggesting that $\Delta I/I_0$ has wider operating concentration range than $\Delta\mu/\mu_0$. Interestingly, among the applied polymers, PDPP-FAF/QCM hybrid sensor has the lowest LOD for most VOCs, while the OFET based on PDPP-FAF has the highest LOD for most VOCs. It suggests that combining different sensing technologies may develop a better understanding of prospects for sensing of materials and screen out suitable techniques toward a specific sensing application.

4. Conclusions

In summary, we have successfully demonstrated the feasibility of DPP based donor-acceptor p-type and ambipolar copolymer thin films as a potential class of active materials for the sensing of aliphatic alkanes and aromatic benzene derivatives via OFET based chemical sensors. The unique chemical structure and assembled nanofiber geometry of DPP based copolymers provide high affinity and large adsorption surface to various alkanes and aromatic compounds, resulting in high sensitivity to these VOCs. In addition, DPP copolymer OFETs can form a sensor array, which possesses an excellent discriminative power between the aliphatic alkanes and aromatic compounds, as well as between different chemical species. These sensing platforms provide a good opportunity to study both the polymer nanostructure morphology and analyte vapor interaction (physisoprtion) and charge transport behavior change upon analyte exposure.

Acknowledgements

The research leading to these results has received finding from the Horizon 2020 ICT Program under the SNIFFPHONE (grant agreement no. 644031). Prashant Sonar is thankful to the Australian Research Council (ARC) for the Future Fellowship (FT130101337) at Queensland University of Technology (QUT). PS is also acknowledges the Visiting Investigatorship Program (VIP), A*STAR, Singapore. S.M. thanks the Ministry of Education of Singapore. We also thank Dr. Amit Jaiswal for reviewing the manuscript.

Appendix A. Supplementary data

Supplementary data associated with this article can be found, in the online version, at http://dx.doi.org/10.1016/j.snb.2017.04.167.

References

[1] L.A. Wallace, Human exposure to volatile organic pollutants: implications for indoor air studies, Annu. Rev. Energy Environ. 26 (2001) 269–301.
[2] R.P. Wayne, Chemistry of Atmospheres, 3rd ed., Oxford University Press, Oxford, UK, 2000.
[3] A.N. Sokolov, B.C. Tee, C.J. Bettinger, J.B. Tok, Z. Bao, Chemical and engineering approaches to enable organic field-effect transistors for electronic skin applications, Acc. Chem. Res. 45 (2012) 361–371.

[4] T. Someya, A. Dodabalapur, J. Huang, K.C. See, H.E. Katz, Chemical and physical sensing by organic field-effect transistors and related devices, Adv. Mater. 22 (2010) 3799–3811.
[5] A.C. Arias, J.D. MacKenzie, I. McCulloch, J. Rivnay, A. Salleo, Materials and applications for large area electronics: solution-based approaches, Chem. Rev. 110 (2010) 3–24.
[6] B. Crone, A. Dodabalapur, A. Gelperin, L. Torsi, H.E. Katz, A.J. Lovinger, et al., Electronic sensing of vapors with organic transistors, Appl. Phys. Lett. 78 (2001) 2229.
[7] A. Bayn, X. Feng, K. Muellen, H. Haick, Field effect transistors based on polycyclic aromatic hydrocarbons for the detection and classification of volatile organic compounds, ACS Appl. Mater. Interfaces 5 (2013) 3431–3440.
[8] Y.S. Jung, W. Jung, H.L. Tuller, C.A. Ross, Nanowire conductive polymer gas sensor patterned using self-assembled block copolymer lithography, Nano Lett. 8 (2008) 3776–3780.
[9] N. Bachar, L. Liberman, F. Muallem, X.L. Feng, K. Mullen, H. Haick, Sensor arrays based on polycyclic aromatic hydrocarbons: chemiresistors versus quartz-crystal microbalance, ACS Appl. Mater. Interfaces 5 (2013) 11641–11653.
[10] P. Lienerth, S. Fall, P. Lévêque, U. Soysal, T. Heiser, Improving the selectivity to polar vapors of OFET-based sensors by using the transfer characteristics hysteresis response, Sens. Actuators B 225 (2016) 90–95.
[11] A.N. Mallya, R. Kottokkaran, P.C. Ramamurthy, Conducting polymer–carbon black nanocomposite sensor for volatile organic compounds and correlating sensor response by molecular dynamics, Sens. Actuators B 201 (2014) 308–320.
[12] D.C. Wedge, A. Das, R. Dost, J. Kettle, M.-B. Madec, J.J. Morrison, et al., Real-time vapour sensing using an OFET-based electronic nose and genetic programming, Sens. Actuators B 143 (2009) 365–372.
[13] L. Li, P. Gao, M. Baumgarten, K. Muellen, N. Lu, H. Fuchs, et al., High performance field-effect ammonia sensors based on a structured ultrathin organic semiconductor film, Adv. Mater. 25 (2013) 3419–3425.
[14] W. Huang, K. Besar, R. LeCover, A.M. Rule, P.N. Breysse, H.E. Katz, Highly sensitive NH_3 detection based on organic field-effect transistors with tris(pentafluorophenyl)borane as receptor, J. Am. Chem. Soc. 134 (2012) 14650–14653.
[15] S. Han, X. Zhuang, W. Shi, X. Yang, L. Li, J. Yu, Poly(3-hexylthiophene)/polystyrene, (P3HT/PS) blends based organic field-effect transistor ammonia gas sensor, Sens. Actuators B 225 (2016) 10–15.
[16] J. Yu, X. Yu, L. Zhang, H. Zeng, Ammonia gas sensor based on pentacene organic field-effect transistor, Sens. Actuators B 173 (2012) 133–138.
[17] D. Gopalakrishnan, W.R. Dichtel, Real-Time, Ultrasensitive detection of RDX vapors using conjugated network polymer thin films, Chem. Mater. 27 (2015) 3813–3816.
[18] S.G. Surya, S.S. Nagarkar, S.K. Ghosh, P. Sonar, V. Ramgopal Rao, OFET based explosive sensors using diketopyrrolopyrrole and metal organic framework composite active channel material, Sens. Actuators B 223 (2016) 114–122.
[19] J. Huang, J. Miragliotta, A. Becknell, H.E. Katz, Hydroxy-terminated organic semiconductor-based field-effect transistors for phosphonate vapor detection, J. Am. Chem. Soc. 129 (2007) 9366–9376.
[20] O.S. Kwon, S.J. Park, J.S. Lee, E. Park, T. Kim, H.-W. Park, et al., Multidimensional conducting polymer nanotubes for ultrasensitive chemical nerve agent sensing, Nano Lett. 12 (2012) 2797–2802.
[21] Y. Qiao, Y. Guo, C. Yu, F. Zhang, W. Xu, Y. Liu, et al., Diketopyrrolopyrrole-containing quinoidal small molecules for high-performance, air-stable, and solution-processable n-channel organic field-effect transistors, J. Am. Chem. Soc. 134 (2012) 4084–4087.
[22] P. Sonar, T.-J. Ha, A. Dodabalapur, A fluorenone based low band gap solution processable copolymer for air stable and high mobility organic field effect transistors, Chem. Commun. 49 (2013) 1588–1590.
[23] P. Sonar, S.P. Singh, E.L. Williams, Y.N. Li, M.S. Soh, A. Dodabalapur, Furan containing diketopyrrolopyrrole copolymers: synthesis, characterization, organic field effect transistor performance and photovoltaic properties, J. Mater. Chem. 22 (2012) 4425–4435.
[24] P. Sonar, T.R.B. Foong, S.P. Singh, Y. Li, A. Dodabalapur, A furan-containing conjugated polymer for high mobility ambipolar organic thin film transistors, Chem. Commun. 48 (2012) 8383–8385.
[25] Y. Li, P. Sonar, L. Murphy, W. Hong, High mobility diketopyrrolopyrrole (DPP)-based organic semiconductor materials for organic thin film transistors and photovoltaics, Energy Environ. Sci. 6 (2013) 1684–1710.
[26] P. Sonar, S.P. Singh, Y.N. Li, Z.E. Ooi, T.J. Ha, I. Wong, et al., High mobility organic thin film transistor and efficient photovoltaic devices using versatile donor-acceptor polymer semiconductor by molecular design, Energy Environ. Sci. 4 (2011) 2288–2296.
[27] Y. Li, S.P. Singh, P. Sonar, A high mobility P-type DPP-thieno 3,2-b thiophene copolymer for organic thin-film transistors, Adv. Mater. 22 (2010) 4862–4866.
[28] J. Bai, Y. Liu, S. Oh, W. Lei, B. Yin, S. Park, et al., A high-performance ambipolar organic field-effect transistor based on a bidirectional [small pi]-extended diketopyrrolopyrrole under ambient conditions, RSC Adv. 5 (2015) 53412–53418.
[29] J. Lee, A.R. Han, J. Kim, Y. Kim, J.H. Oh, C. Yang, Solution-processable ambipolar diketopyrrolopyrrole–selenophene polymer with unprecedentedly high hole and electron mobilities, J. Am. Chem. Soc. 134 (2012) 20713–20721.
[30] H. Bronstein, Z. Chen, R.S. Ashraf, W. Zhang, J. Du, J.R. Durrant, et al., Thieno[3,2-b]thiophene–diketopyrrolopyrrole-containing polymers for high-performance organic field-effect transistors and organic photovoltaic devices, J. Am. Chem. Soc. 133 (2011) 3272–3275.
[31] S.-X. Sun, Y. Huo, M.-M. Li, X. Hu, H.-J. Zhang, Y.-W. Zhang, et al., Understanding the halogenation effects in diketopyrrolopyrrole-based small molecule photovoltaics, ACS Appl. Mater. Interfaces 7 (2015) 19914–19922.
[32] B. Wang, T.P. Huynh, W.W. Wu, N. Hayek, T.T. Do, J.C. Cancilla, et al., A highly sensitive diketopyrrolopyrrole-based ambipolar transistor for selective detection and discrimination of xylene isomers, Adv. Mater. 28 (2016) 4012–4018.
[33] Y. Yang, G.X. Zhang, H.W. Luo, J.J. Yao, Z.T. Liu, D.Q. Zhang, Highly sensitive thin-film field-effect transistor sensor for ammonia with the DPP-bithiophene conjugated polymer entailing thermally cleavable tert-butoxy groups in the side chains, ACS Appl. Mater. Interfaces 8 (2016) 3635–3643.
[34] G.S. Ryu, K.H. Park, W.T. Park, Y.H. Kim, Y.Y. Noh, High-performance diketopyrrolopyrrole-based organic field-effect transistors for flexible gas sensors, Org. Electron. 23 (2015) 76–81.
[35] P. Sonar, S.P. Singh, Y. Li, M.S. Soh, A. Dodabalapur, A low-bandgap diketopyrrolopyrrole-benzothiadiazole-based copolymer for high-mobility ambipolar organic thin-film transistors, Adv. Mater. 22 (2010) 5409–5413.
[36] P. Hohenberg, W. Kohn, Inhomogeneous electron gas, Phys. Rev. B 136 (1964) B864–B871.
[37] W. Kohn, L.J. Sham, Self-consistent equations including exchange and correlation effects, Phys. Rev. 140 (1965) A1133–A1138.
[38] M.J. Frisch, G.W. Trucks, H.B. Schlegel, G.E. Scuseria, M.A. Robb, J.R. Cheeseman, et al., Gaussian 09, Gaussian, Inc., Wallingford, CT, USA, 2009.
[39] J.D. Chai, M. Head-Gordon, Long-range corrected hybrid density functionals with damped atom–atom dispersion corrections, Phys. Chem. Chem. Phys. 10 (2008) 6615–6620.
[40] S. Grimme, Semiempirical GGA-type density functional constructed with a long-range dispersion correction, J. Comput. Chem. 27 (2006) 1787–1799.
[41] P.B. Luppa, L.J. Sokoll, D.W. Chan, Immunosensors – principles and applications to clinical chemistry, Clin. Chim. Acta 314 (2001) 1–26.
[42] K.J. Albert, N.S. Lewis, C.L. Schauer, G.A. Sotzing, S.E. Stitzel, T.P. Vaid, et al., Cross-reactive chemical sensor arrays, Chem. Rev. 100 (2000) 2595–2626.
[43] B. Wang, J.C. Cancilla, J.S. Torrecilla, H. Haick, Artificial sensing intelligence with silicon nanowires for ultraselective detection in the gas phase, Nano Lett. 14 (2014) 933–938.
[44] P.C. Jurs, G.A. Bakken, H.E. McClelland, Computational methods for the analysis of chemical sensor array data from volatile analytes, Chem. Rev. 100 (2000) 2649–2678.
[45] Y. Chen, S. Manzhos, A comparative computational study of lithium and sodium insertion into van der Waals and covalent tetracyanoethylene (TCNE)-based crystals as promising materials for organic lithium and sodium ion batteries, Phys. Chem. Chem. Phys. 18 (2016) 8874–8880.
[46] Y.Q. Chen, S. Manzhos, A computational study of lithium interaction with tetracyanoethylene (TCNE) and tetracyaniquinodimethane (TCNQ) molecules, Phys. Chem. Chem. Phys. 18 (2016) 1470–1477.

Biographies

Dr. Bin Wang received his B.E. degree in Polymer Materials and Engineering from Zhengzhou University in 2004. He received his Ph.D in Polymer Chemistry and Physics from Nankai University in 2010. Since February 2011, Dr. Bin Wang serves as a postdoctoral fellow in the group of Prof. Hossam Haick in Technion – Israel Institute of Technology. His research focuses on the developing organic/inorganic field effect transistor based gas sensors.

Prashant Sonar did his doctoral work at Max-Planck Institute of Polymer Research (Mainz, Germany) and was awarded his PhD in 2004 from Johannes-Gutenberg University in Mainz. After a postdoctoral period in ETH, in 2006, A/Prof. Sonar moved to the Institute of Materials Research and Engineering (IMRE), Agency of Science, Technology and Research (A*STAR), where he served as a Research Scientist. Dr. Sonar recently was appointed as Associate Professor in July 2014 at Queensland University of Technology (QUT), Brisbane, Australia. A/Prof. Sonar is interested in design and synthesis of novel π-functional materials (small molecules, oligomers, dendrimers and polymers) for printed electronics, (OFETs, OLEDs, OPVs, OLETs, OPDs, and Sensors) bioelectronics and supramoleculecular electronic applications.

Dr. Sergei Manzhos is an Assistant Professor at the Department of Mechanical Engineering, Faculty of Engineering, National University of Singapore. His research interests include the theory and computational modeling of processes in photoelectrochemical cells and metal ion batteries, modeling of molecule-surface reactions and vibrational spectroscopy of adsorbed species.

Hossam Haick, Professor at the Technion – Israel Institute of Technology, is an expert in the field of nanotechnology and smart sensors. He is the founder and leader of several European consortiums for the development of advanced generations of nanosensors for disease diagnosis. His research interests include nanomaterial-based chemical (flexible) sensors, electronic skin, nanoarray devices for screening, diagnosis, and monitoring of disease, breath analysis, volatile biomarkers, and molecular electronic devices.